Enhancing Public Safety through Dynamic Switching Between Unicast and Broadcast Transmission Modes in Cellular Networks

Mohamad Younes, Yves Louet

IEEE Access
Multidisciplinary | Rapid Review | Open Access Journal

Received 11 November 2024, accepted 13 December 2024, date of publication 19 December 2024, date of current version 3 January 2025.

Digital Object Identifier 10.1109/ACCESS.2024.3520407

RESEARCH ARTICLE

Enhancing Public Safety Through Dynamic Switching Between Unicast and Broadcast Transmission Modes in Cellular Networks

MOHAMAD YOUNES[1] AND YVES LOUËT[2], (Senior Member, IEEE)
[1]Centre de Recherche de Coëtquidan, Académie Militaire de Saint-Cyr Coëtquidan, 56380 Guer, France
[2]CentraleSupélec, Campus de Rennes, IETR, 35557 Cesson-Sévigné, France

Corresponding author: Mohamad Younes (Mohamad.younes@st-cyr.terre-net.defense.gouv.fr)

ABSTRACT This article proposes new directions to enhance spectrum resource allocation in dense cellular networks, especially during massive dissemination of public safety alerts. We are conducting a comparative study to identify the most efficient transmission mode among the following options: conventional Unicast (UC) mode, UC mode combined with beamforming, Point-To-Multipoint (PTM) single-cell broadcast mode, and multi-cell broadcast mode via a Single-Frequency Network (SFN). In the absence of standardized norms for determining the optimum mode, we are developing a model to establish a threshold for the number of users per base station, at which point each broadcast mode between SFN and PTM becomes more spectrally efficient than conventional UC and UC with beamforming. Our contribution includes an in-depth simulation study to assess the sensitivity of this threshold to the variability of system parameters under different scenarios and conditions. This analysis will support informed decisions on the optimal transmission mode, thereby improving public safety in critical circumstances.

INDEX TERMS Beamforming, mass distribution of alert content, PTM, SFN, spectrum resource allocation, UC.

I. INTRODUCTION

The needs of mobile broadband users have evolved considerably in recent years, demanding massive connectivity, increased reliability, minimal latency, high data rates and support for new device types [1], [2], [3]. To meet these growing requirements, 5G technology offers three main types of service: enhanced mobile broadband, ultra-reliable low-latency communications, and massive machine-type communications [4], [5]. However, despite these advances, the simultaneous and massive dissemination of content, such as real-time alerts, remains a major challenge. In crisis situations, it is crucial to ensure rapid, reliable transmission of such information to guarantee public safety. This relies on effective coordination between human actors (security guards, law enforcement agencies, civilians) and cooperation between Base Stations (BSs), to ensure the smooth exchange of critical information. Therein lies the central challenge of this article: to overcome the limitations of current solutions and identify optimized transmission modes that meet the specific constraints of mass dissemination in emergency situations.

In crisis situations, connection quality is closely linked to the density and position of BSs, two key elements for reducing interference and minimizing signal attenuation [6], [7]. To model these complex environments, stochastic geometry proves to be a relevant approach, taking into account the random distribution of BSs and users to estimate key performance indicators such as outage probability, Signal-to-Interference-plus-Noise Ratio (SINR), and both spectral and energy efficiency [8], [9]. These indicators can be used to assess a network's ability to cope with saturation problems, particularly in densely populated areas where the densification of BSs intensifies inter-cell interference [10], [11], [12], [13].

In this context, the choice of BS transmission mode is of paramount importance in limiting saturation. Multicast/broadcast transmission modes appear to be promising

The associate editor coordinating the review of this manuscript and approving it for publication was Tiago Cruz.

alternatives to Unicast (UC) mode, enabling simultaneous and rapid dissemination of content on the same frequency [1], [14], [15], [16], [17], [18]. Nevertheless, UC mode, favored for personalized communications, raises the question of the most suitable transmission strategy depending on the context [19], [20], [21], [22]. Our study therefore explores the extent to which the choice between different transmission modes can optimize information dissemination in times of crisis, taking into account saturation constraints and the need for rapid and reliable dissemination.

The Multicast/Broadcast Multimedia Services (MBMS) specification defines two approaches to multicast/broadcast transmission: the Point-To-Multipoint (PTM) single-cell mode and the multi-cell mode via a Single-Frequency Network (SFN) [14], [23], [24], [25], [26]. The latter requires precise synchronization of the BSs to transmit the same content simultaneously, which reduces interference and improves coverage. In contrast, the more flexible PTM mode allows each BS to transmit independently, thus simplifying its implementation, but at the cost of less interference reduction. With this in mind, the article takes an in-depth look at the advantages and limitations of each transmission mode for large-scale content delivery.

This study builds on previous work published in [27], where we compared UC and SFN modes in terms of spectral resource allocation. In this extension, we extend the analysis to include a diversity of transmission modes: conventional UC, UC with beamforming, PTM and SFN, applied to more varied scenarios. Although only a few studies have previously compared PTM and SFN modes using the same bandwidth [14], [28], [29], [30], our study differs in several respects. Firstly, it is based on the assumption that BSs transmit the same downlink content via the different modes, on the same carrier frequency and in the same bandwidth. In addition, our study explores the potential advantages of using UC mode with beamforming over conventional UC mode.

To the best of our knowledge, the literature is still very limited when it comes to comparing broadcast modes (PTM and SFN) and UC mode with beamforming in scenarios where BSs are randomly distributed and transmit the same content. Some studies have already shown the superiority of PTM mode in different contexts [28], [31], including regular hexagonal patterns or configurations with a low density of BSs equipped with omnidirectional antennas. However, optimizing resource allocation to guarantee ultra-reliable connectivity for security has not yet been thoroughly analyzed. This complexity is accentuated by the absence, to date, of a standardized norm recognized as optimal in terms of resource allocation in the context of mass broadcasting, a challenge to which this article aims to provide an answer.

To ensure reliable results, our study is based on assumptions similar to those of real deployments, taking into account the effects of transmission channel modeling according to the 3rd Generation Partnership Project (3GPP) reference model [32], as well as characteristics such as high density, tri-sectorization and random distribution of BSs in the study area. We also take into account inter- and intra-cell interference, given their significant impact on signal quality and spectral resource allocation. In addition, we propose expressions for determining a critical cell load threshold, corresponding to the number of users per BS beyond which broadcast transmission modes, notably PTM and SFN, outperform UC mode (with and without beamforming) in terms of spectrum resource allocation efficiency. Our analysis also examines the robustness of this threshold in the face of variations in several system parameters, such as channel conditions, random BS locations, BS densities and transmission power, number of beamforming antennas, SFN zone size, and required coverage probability.

By analyzing the stability of this threshold as a function of these different parameters, our study aims to propose practical recommendations for optimizing mass transmission in crisis situations. It thus provides concrete elements for improving Quality of Service (QoS) and spectrum resource management in mass networks, offering a solid basis for guiding transmission mode choices in critical contexts where speed and reliability are paramount.

The remainder of this article is organized as follows. In Section II, we review the state-of-the-art in MBMS technologies and MBMS operation on-Demand (MooD), with particular emphasis on switching between transmission modes. Section III covers the channel model and SINR calculation for conventional UC, UC with beamforming, as well as PTM and SFN broadcast modes. Section IV focuses on allocation of resources needed to meet service providers' QoS requirements, for the various transmission modes. Next, we propose expressions to determine a threshold relative to the number of users per BS beyond which switching from UC (with and without beamforming) to broadcast mode (SFN or PTM) becomes necessary. Section V presents the numerical results of simulations examining the impact of various system parameters on coverage and the switching threshold under different conditions. Finally, Section VI summarizes the article's conclusions.

II. STATE-OF-THE-ART ON THE EVOLUTION OF MBMS TECHNOLOGIES FOR CELLULAR NETWORKS

Initially designed by the 3GPP standards bodies, MBMS was intended to support multimedia services on 3G networks [33]. With the move to 4G Long-Term Evolution (LTE) and evolved MBMS (eMBMS), 3GPP releases 8 and 9 introduced the SFN broadcast transmission technique. Thanks to the significant reduction in interference via SFN, this mode can be used to transmit content to mass users over a wide coverage area, including large cities [34].

In SFN broadcasting, a user receives several copies of the same signal from different transmitting BSs in the SFN area, with different propagation delays. The user's equipment can combine these copies constructively, thus improving the QoS of the received signal [26]. However, time synchronization is a major challenge for SFN deployment [30]. Perfect

synchronization of the BS clocks is required, with a variance in time synchronization well below the cyclic prefix time interval, on the order of microseconds. Nevertheless, the recent development of time synchronization technologies, such as Global Positioning System (GPS) time synchronization [35], widely used in Internet of Things (IoT) devices and localization, facilitates this synchronization and can greatly contribute to SFN deployment [30].

In addition, to overcome the limitations of SFN mode, which requires a group of BSs to broadcast, 3GPP has introduced PTM mode. PTM enables more targeted broadcasting within a single BS. PTM features have been integrated into 4G LTE-Advanced Pro releases 13 and 14 to support a variety of services, including digital TV, machine-to-machine communications, mission-critical communications, and vehicular communications [30], [36], [37]. In addition, in [26], the authors examined the enhancements to eMBMS provided by the PTM mode, highlighting its ability to facilitate group communication services. This mode also offers a more flexible approach by allowing dynamic use of time and frequency resources, even within a subframe [38]. This flexibility is particularly useful for broadcast services covering restricted geographical areas, such as hotspots, within a single BS.

In line with efforts to optimize broadcast services, 3GPP releases 14 and 15 have brought improvements by dedicating a specific carrier to MBMS transmission. This initiative aims to maximize resource utilization, offering the possibility of exploiting up to 100% of the capacity dedicated to MBMS. Moreover, the addition of a long-duration Orthogonal Frequency-Division Multiplexing (OFDM) symbol plays a crucial role in extending the coverage range, which can reach several tens of kilometers [38].

Furthermore, 3GPP version 16 introduced terrestrial broadcast technology, which aims to enhance the broadcasting of television services over large static transmission areas, using specific infrastructures such as High-Power High-Tower (HPHT) [39], [40], [41]. These advances represent an extension of LTE to provide enhanced PTM capabilities in release 16, meeting the multimedia broadcasting needs of 5G [42], [43].

Furthermore, 3GPP releases 16 and 17 have introduced a new feature called mixed mode multicasting for 5G. This feature enables dynamic switching between UC and PTM transmission modes, offering integrated optimization possibilities in the Radio Access Network (RAN). In addition, it offers configurable and dynamic coverage, extending from a single cell to a large area, opening up promising prospects for the provision of multimedia services with identical content over the RAN [36].

In this context, a key 3GPP requirement is to provide a flexible service based on dynamic switching in response to changing conditions, thanks to the introduction of MooD [19]. Significant progress has been made in eMBMS with the integration of MooD functionalities, standardized in 3GPP release 12 for LTE networks. These features are detailed in Technical Report (TR) 26.849 [44] and Technical Specification (TS) 26.346 [45], enabling the dynamic creation of MBMS services in response to actual user demand. Thus, when a service or content, normally provided in UC mode, arouses simultaneous demand from several users, the network can set up a user service in broadcast mode to relieve the network in UC mode [19]. By subsequently adjusting the distribution mode when demand falls below a pre-configured threshold, switching from broadcast to UC mode, this solution optimizes the use of network resources [19], [36], [41].

It is essential to emphasize that dynamic transmission mode selection (via MooD) is not limited to an individual solution, but rather constitutes an integrated set of tools, procedures and best practices used at different system levels to ensure efficient multicast/broadcast transmission. This process of dynamic multicast/broadcast switching involves two distinct stages, as described in [46]. The first step consists of converting the content into a format suitable for multicast/broadcast mode, usually using the corresponding Internet Protocol (IP) transport. Then, the second step entails optimizing RAN resources by selecting the most appropriate transmission mode from among those available, for mass distribution of content to users.

In line with these advances, in [47] it is proposed to explore two distinct approaches to improving the use of eMBMS and Group Communication System Enablers (GCSE) [48]. The first approach, called static eMBMS activation, mainly favors multicast mode, while UC mode is configured as a backup solution. In contrast, the second approach, called dynamic eMBMS activation, initially based on UC mode, automatically switches to multicast mode as soon as a certain number of group members is reached.

In comparison with previous work on MooD operation, our study introduces a new approach to switching between different transmission modes, including the threshold number of users per BS beyond which each broadcast mode (SFN or PTM) becomes more efficient than the UC mode (with and without beamforming).

III. CHANNEL MODEL AND SINR CALCULATION

In the context of realistic modeling of dense cellular networks, characterized by a random distribution of BS locations, our evaluation is based on the assumption that BSs are tri-sectoral and randomly distributed at high density over a square-shaped geographical area following a Poisson Point Process (PPP) distribution. This distribution is characterized by a single parameter: the BS density, expressed as the number of BSs per unit km^2.

Moreover, the outage probability (p_o) emerges as an essential performance metric, quantifying the probability that a received signal is below a specific threshold with respect to noise and interference levels [49]. In our study, we define p_o as the probability that the SINR (γ) is below a predefined threshold (T), also known as the SINR target. This measure is expressed as: $p_o = P\{\gamma < T\}$, and is equivalent to defining

the probability of coverage as: $p_c = P\{\gamma \geq T\}$. Note that the predefined threshold T represents the SINR value where maximum signal power loss is tolerable while maintaining a reliable wireless connection. We therefore take T into account when evaluating the coverage p_c in the different modes, while exploring the sensitivity of p_c to the variability of system parameters.

A. CHANNEL MODEL

We model the transmission channel, taking into account the effects of path loss, fading and shadowing in accordance with the model established by the 3GPP [32].

To express path loss between a BS and a user r meters apart, we use the formula $= r^{\alpha}/\kappa$, where κ represents the path loss factor and α the path loss exponent. Let us then reformulate L in dB: $L\,[dB] = 10\alpha log_{10}(r) - 10log_{10}(\kappa)$. The values of α and κ can be determined using (1), applicable to f_c between 1.4 GHz and 2.6 GHz [32], which is as follows:

$$\begin{aligned} L\,[dB] &= 128.1 + 37.6log_{10}\,(R) + 21log_{10}\left(\frac{f_c}{2}\right) \\ &= 15.3 + 37.6log_{10}\,(r) + 21log_{10}\left(\frac{f_c}{2}\right), \end{aligned} \quad (1)$$

where R is the distance between the BS and the user in km ($R = \frac{r}{10^3}$), and f_c is expressed in GHz. By identification, we obtain: $\alpha = 3.76$ and $\kappa = 10^{-\left(1.53+2.1log_{10}\left(\frac{f_c}{2}\right)\right)}$. For the rest of the article, we consider three values of f_c: 1.6 GHz, 2 GHz, and 2.4 GHz, i.e. κ values of 0.0472, 0.0295, and 0.0201 respectively.

The fading factor, noted h in the following, is considered to be a random variable following an exponential distribution with a unit mean. As for the shadowing parameter, it is modeled using a lognormal random variable, denoted $e^{\chi_{c,i}}$, where $\chi_{c,i}$ is defined by its standard deviation $\sigma = \frac{10}{\sigma_{dB} ln(10)}$. In this work, we take into account obstacles close to the receiver (denoted by χ_c) as well as independent obstacles for each BS (denoted by χ_i), so that:

$$\chi_{c,i} = \chi_c + \chi_i. \quad (2)$$

In order to attribute the same impact to obstacles on the transmitting and receiving sides, we assume that: $\sigma_c^2 = \sigma_i^2 = \frac{\sigma^2}{2}$, where σ_c and σ_i represent the standard deviation of χ_c and χ_i respectively.

Now considering a user located at a distance $r_{c,i}$ from a certain base station (BS_i) transmitting with a power of P_{tx}, we can express the received signal power in UC and PTM modes as a function of the path loss exponent α, the fading factor h_i, and the shadowing parameter $e^{\chi_{c,i}}$, as follows:

$$P_r = MP_{tx}\kappa r_{c,i}^{-\alpha} e^{\chi_{c,i}} h_i G\left(\theta_{i,t}\right), \quad (3)$$

where M represents the number of antennas per sector of tri-sector BSs (with $M = 1$ in conventional UC and PTM modes, and $M > 1$ in UC mode with beamforming), sub-index i denotes the BS_i, sub-index t denotes the service sector of the BS_i, and $G\left(\theta_{i,t}\right)$ is the antenna gain in the $\theta_{i,t}$ direction, calculated in dB according to 3GPP specifications as follows [32]:

$$G\left(\theta_{i,t}\right)_{dB} = G_A - min\left\{12\left(\frac{\theta_{i,t}}{\theta_{3dB}}\right)^2, G_{FB}\right\}, \quad (4)$$

where G_A is the antenna gain in the boresight direction in dB, G_{FB} is the front-to-back ratio of the antenna, θ_{3dB} is the beamwidth at 3 dB, and $-180° \leq \theta_{i,t} \leq 180°$.

Taking into account the shadowing parameters χ_c and χ_i, we can re-express the power P_r of the signal received from BS_i as follows:

$$P_r = MP_{tx}\kappa r_{c,i}^{-\alpha} e^{\chi_c} e^{\chi_i} h_i G\left(\theta_{i,t}\right). \quad (5)$$

Now let us posit $r_i = r_{c,i}.e^{-\frac{\chi_i}{\alpha}}$ as the modified distance between the user and BS_i, obtained by taking into account the effect of the obstacle close to BS_i (χ_i) on the actual distance between the user and $BS_i(r_{c,i})$, we obtain:

$$P_r = MP_{tx}\kappa r_i^{-\alpha} e^{\chi_c} h_i G\left(\theta_{i,t}\right). \quad (6)$$

This change in distance (from $r_{c,i}$ to r_i) can be seen as a change in the initial location of BS_i.

B. CALCULATION OF SINR IN UC (WITH AND WITHOUT BEAMFORMING) AND PTM MODES

For UC (with and without beamforming) and PTM modes, characterized by independent transmissions at the level of each BS, as opposed to the SFN mode characterized by inter-cell cooperative transmissions, we make the assumption that only the service BS (BS_s) contributes to the useful signal power, even though it's not necessarily the one closest to the user. On the other hand, all other BSs in the study area generate interference. Thus, the received useful signal power (P_r) of BS_s in UC and PTM modes, is expressed as follows:

$$P_s = MP_{tx}\kappa r_s^{-\alpha} e^{\chi_c} h_s G\left(\theta_{s,t}\right). \quad (7)$$

where the sub-index s denotes the BS_s and the sub-index t denotes the service sector of the BS_s, while considering that M is equal to 1 in the conventional UC and PTM modes, and greater than 1 in the UC mode with beamforming.

The evaluation of interference power in UC and PTM modes is carried out taking into account two distinct components. The first component (I_s) is related to the other two sectors of BS_s and is calculated as follows:

$$I_s = P_{tx}\kappa r_s^{-\alpha} e^{\chi_c} h_s \sum_{j=1/j\neq t}^{3} X_{s,j}, \quad (8)$$

where sub-index j represents the interference sectors of BS_s, i.e. with condition $j \neq t$ where t represents the service sector of BS_s. Note that $X_{s,j}$ is defined in conventional UC and PTM modes by the antenna gain $G\left(\theta_{s,j}\right)$, and in UC mode with beamforming by the gain of the beamforming network $A\left(\theta_{s,j}, \emptyset_{s,j}\right)$. Finally, $A\,(\theta, \emptyset)$ representing the beamforming network gain for a sector in the θ direction is defined as

follows [50]:

$$A(\theta, \emptyset) = \begin{cases} \dfrac{sin^2\left(M\frac{\pi}{2}\left(sin(\emptyset) - sin(\theta)\right)\right)}{M sin^2\left(\frac{\pi}{2}\left(sin(\emptyset) - sin(\theta)\right)\right)} & G(\theta),\ \theta \neq \emptyset \\ MG(\theta),\ \theta = \emptyset, \end{cases} \tag{9}$$

where $G(\theta)$ is given by (4) and $-60° \leq \emptyset \leq 60°$. Note that antenna orientation is determined as a function of an orientation angle $\emptyset$ measured from the antenna's boresight axis.

Let us now turn to the expression of the second component of the interference power in the UC (with and without beamforming) and PTM modes. This component ($I_{i\in\psi/i\neq s}$) is associated with the other BSs in the study area and is calculated as follows:

$$I_{i\in\psi/i\neq s} = P_{tx}\kappa e^{\chi_c} \sum\nolimits_{i\in\psi/i\neq s} r_i^{-\alpha} h_i \sum\nolimits_{j=1}^{3} X_{i,j}, \tag{10}$$

where sub-index i denotes interference-generating BSs, and ψ is the set of all BSs distributed in the study area according to PPP. Let us note that i belongs to the set ψ, with the exception of the service BS BS_s, and therefore with the condition $i \neq s$. Note that $X_{i,j}$ is defined in conventional UC and PTM modes by the antenna gain $G\left(\theta_{i,j}\right)$, and in UC mode with beamforming by the gain of the beamforming network $A\left(\theta_{i,j}, \emptyset_{i,j}\right)$, as described in (4) and (9) respectively.

Consequently, the SINR (γ) in UC and PTM modes is expressed as the ratio between the received signal power (P_r) and the sum of the interference signal powers (I_s and $I_{i\in\psi/i\neq s}$) and the noise power at the receiver (P_N), as follows:

$$\gamma = \frac{P_r}{P_N + I_r} = \frac{P_r}{P_N + I_s + I_{i\in\psi/i\neq s}}, \tag{11}$$

with:

$$P_N\,[\text{dBW}] = NF + 10log_{10}\left(KT_K B\right), \tag{12}$$

where K is Boltzmann's constant, T_K is the receiver system temperature, NF is the receiver noise figure in dB, and B is the bandwidth.

C. CALCULATION OF SINR IN SFN MODE

As a reminder, SFN mode, characterized by synchronous multicell transmission, involves a group of BSs simultaneously broadcasting the same signal in the SFN zone [33]. This approach favors efficient broadcasting of the same content, thanks to synchronized transmission by a group of BSs using the same carrier frequency (f_c) and bandwidth (B). Thus, when a user receives a signal transmitted by a BS different from the service BS BS_s, noted BS_i, this signal reaches the user with a certain delay ($\Delta\tau$). This delay is calculated as a function of the distances between the user and the base stations BS_s and BS_i, noted r_s and r_i respectively, as well as the speed of light c, according to the following formula:

$$\Delta\tau = \frac{r_i - r_s}{c}. \tag{13}$$

The time offset $\Delta\tau$ plays a decisive role in determining the contribution rate to the useful power received (δ_i), whose value varies between 0 and 1. Depending on the value of $\Delta\tau$, three scenarios can occur:

- If $\Delta\tau$ is less than or equal to the guard interval (T_g), there is no interference, and δ_i is equal to 1.
- If $\Delta\tau$ is greater than T_g and less than or equal to the total OFDM symbol duration (T_f), where T_f is defined as the sum of the useful symbol duration (T_u) and T_g, i.e. $T_f = T_g + T_u$, then δ_i varies between 0 and 1.
- If $\Delta\tau$ is greater than T_f, there is no contribution to the useful power received, and so δ_i is equal to 0.

Thus, the expression of δ_i taking into account BS_i is defined as follows:

$$\delta_i = \begin{cases} 1 & 0 \leq \Delta\tau \leq T_g \\ \left(\dfrac{T_u - \Delta\tau + T_g}{T_u}\right)^2 & T_g < \Delta\tau \leq T_f \\ 0 & \Delta\tau > T_f. \end{cases} \tag{14}$$

In the remainder of the article, N_{BS} is used to denote the total number of BSs in the study area. We also define N_{SFN} as equal to ρN_{BS} (where ρ is the normalized size of the SFN zone, $0 < \rho \leq 1$), representing the number of BSs located around the center of the study area participating in the SFN synchronized transmission. Consequently, the total power received from the N_{SFN} BSs in the SFN zone is calculated as follows:

$$P_{SFN}^{in} = P_{tx}\kappa e^{\chi} \sum\nolimits_{i=1}^{N_{SFN}} \delta_i r_i^{-\alpha} h_i \sum\nolimits_{j=1}^{3} G\left(\theta_{i,j}\right), \tag{15}$$

where δ_i represents the weight function for each BS participating in the SFN transmission, calculated according to (14), and sub-indices i and j correspond to the N_{SFN} BSs in the SFN zone and their respective sectors.

For interference power in SFN mode, we take into account its decomposition into two parts. The first component, I_{SFN}^{in}, takes into account the BSs in the SFN zone, which can also cause interference due to delayed signals in this zone. This first I_{SFN}^{in} component is calculated as follows:

$$I_{SFN}^{in} = P_{tx}e^{\chi_c}\kappa \sum\nolimits_{i=1}^{N_{SFN}} (1 - \delta_i) r_i^{-\alpha} h_i \sum\nolimits_{j=1}^{3} G\left(\theta_{i,j}\right). \tag{16}$$

The second component, I_{SFN}^{out}, takes into account BSs outside the SFN zone. This component is calculated as follows:

$$I_{SFN}^{out} = P_{tx}e^{\chi_c}\kappa \sum\nolimits_{i\in\psi/i>N_{SFN}} r_i^{-\alpha} h_i \sum\nolimits_{j=1}^{3} G\left(\theta_{i,j}\right). \tag{17}$$

Thus, the SINR in SFN mode is calculated by:

$$\gamma_{SFN} = \frac{P_{SFN}^{in}}{I_{SFN}^{in} + I_{SFN}^{out} + P_N}. \tag{18}$$

IV. SPECTRUM RESOURCE ALLOCATION WITH A FOCUS ON SWITCHING BETWEEN TRANSMISSION MODES

In this section, we address two key points: calculating the average number of resource blocks allocated in UC (with and without beamforming) and broadcast (SFN and PTM)

modes, and determining the user threshold at which broadcast modes becomes more advantageous than UC mode in terms of resource allocation.

A. CALCULATION OF THE NUMBER OF USERS PER BS FOR SWITCHING FROM UC MODE TO PTM

We start by determining the system capacity and the average number of spectral resource blocks allocated to a user to ensure QoS-compliant reception in UC and PTM modes. In UC mode, the capacity is derived from Shannon's theorem as a function of SINR (γ_{UC}) and bandwidth (B), as follows:

$$C_{UC} = Blog_2\left(1+\gamma_{UC}\right) = N_{UC}^{RB} B_{RB} log_2\left(1+\gamma_{UC}\right), \quad (19)$$

where N_{UC}^{RB} is the number of resource blocks required to access the service and B_{RB} is the bandwidth occupied by a resource block. Thus, to meet users' QoS requirements, the strategy generally adopted is defined by the condition:

$$C_{UC} = N_{UC}^{RB} C_{UC}^{RB} \geq C_{req}, \quad (20)$$

where C_{req} is the capacity required to access the service and $C_{UC}^{RB} = B_{RB} log_2(1+\gamma_{UC})$ is the capacity of a resource block in UC mode.

Let us now focus on calculating the average number of spectral resource blocks allocated in UC and PTM modes. In UC mode, the SINR (γ_{UC}) is calculated for each simulation corresponding to a random distribution of BS locations according to the PPP law. Then, the average number of resource blocks required per user is determined by averaging all γ_{UC} values, from the lowest SINR (γ_{UC}^0) to the highest SINR, as follows:

$$\begin{aligned} N_{UC}^{\bar{RB}} &= \mathbb{E}\left[\frac{C_{req}}{C_{UC}^{RB}}\middle|\, \gamma_{UC} \geq \gamma_{UC}^0\right] \\ &= \frac{C_{req}}{B_{RB}}\mathbb{E}\left[\frac{1}{log_2\left(1+\gamma_{UC}\right)}\middle|\, \gamma_{UC} \geq \gamma_{UC}^0\right]. \end{aligned} \quad (21)$$

In our study, the minimum SINR (γ_{UC}^0) is conceptually equivalent to the 10$^{\text{th}}$ percentile, unless otherwise specified. This parameter evaluates the quality of coverage under unfavorable performance conditions. The 10$^{\text{th}}$ percentile represents the value below which the worst 10% of SINR values fall. In other words, the 10$^{\text{th}}$ percentile measures the least favorable SINR among the 90% of users with the best channel conditions.

Next, we calculate the number of resource blocks allocated in PTM mode, and establish the user threshold above which switching from UC to PTM mode becomes imperative for a more efficient use of the system's spectrum resources.

PTM mode is distinguished by broadcasting from a single BS, where the target SINR level (γ_{SC}^0) is determined to meet a specific coverage requirement (typically 90% in our study, unless otherwise specified). The required capacity in PTM mode (C_{SC}^0) to guarantee access to the service is constant regardless of the number of users and is calculated as follows:

$$C_{SC}^0 = B_{RB} log_2(1+\gamma_{SC}^0). \quad (22)$$

Consequently, the number of resource blocks required in PTM mode to guarantee correct service reception is calculated by:

$$N_{SC}^{RB} = \frac{C_{req}}{C_{SC}^0} = \frac{C_{req}}{B_{RB}} \frac{1}{log_2(1+\gamma_{SC}^0)}. \quad (23)$$

Now let us focus on defining the switching threshold, taking into account the random distribution of BSs in the study area. This threshold represents the number of users per BS above which PTM mode becomes more efficient than UC mode in terms of resource allocation, and can be formulated as follows:

$$N_{UC/SC} = \frac{N_{SC}^{RB}}{N_{UC}^{\bar{RB}}} = \frac{\frac{1}{log_2(1+\gamma_{SC}^0)}}{\mathbb{E}\left[\frac{1}{log_2(1+\gamma_{UC})}\middle|\, \gamma_{UC} \geq \gamma_{UC}^0\right]}. \quad (24)$$

Let us imagine a realistic scenario where a live stream is initially transmitted in UC mode to a small number of users. When this content gains in popularity and the number of users reaches the $N_{UC/SC}$, the MooD is activated. The network then automatically switches to PTM mode to optimize overall use of system resources and guarantee the QoS required by service providers. This transition is transparent to users, with no interruption during content delivery. Then, as the popularity of the content wanes, the network automatically switches back to UC mode, ensuring seamless reception of content for end users.

B. CALCULATION OF THE NUMBER OF USERS PER BS FOR SWITCHING FROM UC MODE TO SFN

Like PTM mode, SFN mode aims to ensure reliable connectivity for users facing the most difficult channel conditions. Consequently, the target capacity for SFN mode is evaluated on the basis of the least favorable performance, thus guaranteeing a sufficient level of SINR for correct service reception. The required capacity of an SFN mode resource block (C_{SFN}^0) is calculated as follows:

$$C_{SFN}^0 = B_{RB} log_2(1+\gamma_{SFN}^0), \quad (25)$$

where γ_{SFN}^0 represents the worst-case SINR among the 90% (unless otherwise specified) of users with the best channel conditions. Consequently, the number of resource blocks allocated in SFN mode is calculated as the ratio between the required capacity (C_{req}) and the worst-case capacity in SFN mode (C_{SFN}^0), as follows:

$$N_{SFN}^{RB} = \frac{C_{req}}{C_{SFN}^0} = \frac{C_{req}}{B_{RB}} \frac{1}{log_2(1+\gamma_{SFN}^0)}. \quad (26)$$

Finally, the number of users for switching from UC mode to SFN mode, taking into account the random location of the BSs, is calculated as follows:

$$N_{UC/SFN} = \frac{N_{SFN}^{RB}}{N_{UC}^{\bar{RB}}} = \frac{\frac{1}{log_2(1+\gamma_{SFN}^0)}}{E\left[\frac{1}{log_2(1+\gamma_{UC})}\middle|\, \gamma_{UC} \geq \gamma_{UC}^0\right]}. \quad (27)$$

The next section presents an in-depth analysis of the thresholds for switching between UC mode (with and without beamforming) and PTM or SFN broadcast mode in various scenarios. This approach, developed in response to 3GPP's MooD, facilitates a dynamic transition between transmission modes, enabling real-time adaptation to changing demand and operational conditions. The results of this study aim to provide substantial value to mobile network operators, guiding them in making informed decisions to ensure reliable and efficient transmission of alert content in hazardous situations.

V. SIMULATION RESULTS

This section presents an in-depth comparative study of conventional UC, UC with beamforming, PTM, and SFN transmission modes, based on 10^4 Monte Carlo simulations. Each simulation generates a new random distribution of BS locations in a 20 km^2 square area, following a PPP-type distribution. In particular, the analysis focuses on a scenario in which the BSs in the study area massively downlink the same content in the different modes. It should be noted that this downlink is carried out taking into account the same transmission power (P_{tx}), the same bandwidth (B) and the same carrier frequency (f_c).

A. COVERAGE PROBABILITY FOR CONVENTIONAL UC AND SFN TRANSMISSION MODES

Recall that the path loss parameters, represented by α and κ, are determined for different values of f_c, in accordance with 3GPP model specifications [32]. For the calculation of noise power (P_N), we consider a noise figure (NF) of 9 dB, a temperature (T_K) of 300 K, and a bandwidth (B) of 5 MHz. In addition, the δ_i function is evaluated considering a guard interval (T_g) of 16.67 μs and a useful symbol duration (T_u) of 66.7 μs. Finally, the antenna gain $G(\theta)$ is calculated with an antenna gain in the boresight direction (G_A) of 15 dBi, an antenna front-to-back ratio (G_{FB}) of 20 dBi, and a 3 dB beamwidth (θ_{3dB}) of 65°.

Our study begins by analyzing the coverage probability (p_c), which represents the percentage of users with an SINR above a predefined threshold (T), also known as the SINR target. Fig. 1 illustrates the variation of p_c as a function of T for conventional UC and SFN transmission modes. The aim of this analysis is to assess the impact of inter-cellular cooperation in SFN mode when distributing alert content, compared with transmission in conventional UC mode. At the same time, to gain a deeper understanding of p_c variability, Fig. 2 and 3 examine the average power of the received useful signal and the average power of interference signals, respectively. These results were obtained for two BS density values: $\lambda = 0.25$ BS/km^2 and $\lambda = 2$ BS/km^2, and for three carrier frequency values: $f_c = 1{,}6$ GHz, 2 GHz and 2,4 GHz. These simulations take into account an SFN zone that covers the entire study area, with a normalized size of $\rho = \frac{N_{SFN}}{N_{BS}} = 1$, where N_{BS} is the total number of BSs in the study area

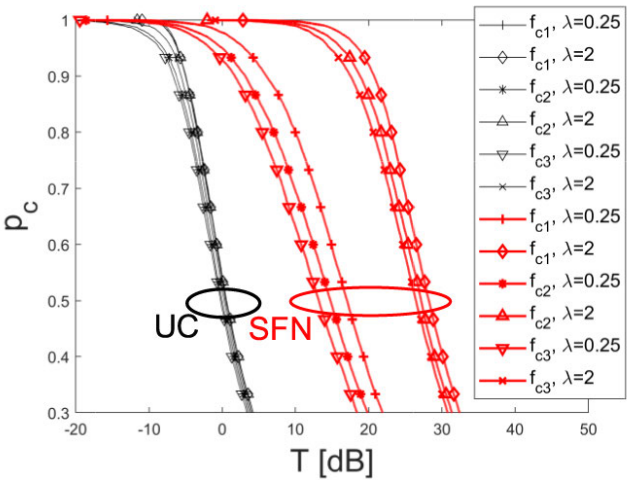

FIGURE 1. Coverage probability (p_c) in UC and SFN modes, as a function of target SINR (T), for transmission power $P_{tx} = 0.5$ W, two BS density values $\lambda = 0.25$ BS/km^2 and 2 BS/km^2, and three carrier frequencies ($f_{c1} = 1.6$ GHz, $f_{c2} = 2$ GHz, and $f_{c3} = 2.4$ GHz).

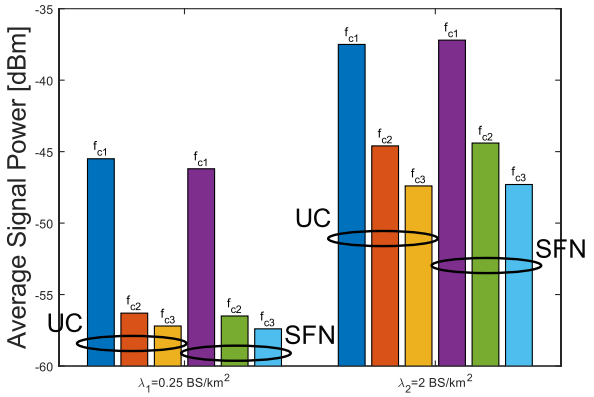

FIGURE 2. Average power of the useful signal received in UC and SFN modes, for a transmission power $P_{tx} = 0.5$ W, two BS density values $\lambda = 0.25$ BS/km^2 and 2 BS/km^2, and three carrier frequencies ($f_{c1} = 1.6$ GHz, $f_{c2} = 2$ GHz, and $f_{c3} = 2.4$ GHz).

and N_{SFN} is the number of BSs located around the origin constituting the SFN zone.

Fig. 1 clearly shows the decrease in p_c in UC and SFN modes as the SINR target (T) increases. The main reason for this trend is that, for high T requirements, the quality of the received signal may not meet the required quality criteria due to inter- and intra-cellular interference. Comparing p_c between UC and SFN modes, we see that SFN mode offers extensive coverage over the whole range of T values, whereas UC mode is more limited. In fact, although both modes have a relatively similar average received useful signal power (see Fig. 2) for the same f_c and λ values, the average interference signal power is significantly lower in SFN mode (see Fig. 3). This disparity leads to an improvement in SINR in SFN mode compared to UC mode, although the values of f_c and λ are identical between the two modes.

Turning now to analysis of the impact of f_c on p_c in Fig. 1, it's worth noting that as f_c increases from 1.6 GHz

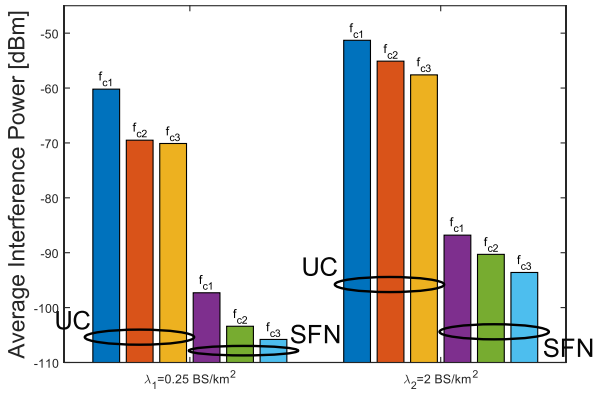

FIGURE 3. Average power of interference signals in UC and SFN modes, for transmission power P_{tx} = 0.5 W, two BS density values λ = 0.25 BS/km^2 and 2 BS/km^2, and three carrier frequencies (f_{c1} = 1.6 GHz, f_{c2} = 2 GHz, and f_{c3} = 2.4 GHz).

to 2 GHz and then to 2.4 GHz, a slight decrease in p_c is observed for both values of λ taken into account. This trend can be explained by the fact that, in both transmission modes, the average power of the received useful signal decreases in line with the decrease in the average power of the interfering signals (see Fig. 2 and 3), thus maintaining a certain constancy in the SINR. This stability is reflected in a limited variation in p_c when f_c is modified.

With regard to the increase in λ from 0.25 BS/km^2 to 2 BS/km^2, the results in Fig. 1 show that this variation does not significantly affect p_c in UC mode. This observation can be explained by the fact that the average power of the received useful signal increases in a manner comparable to the increase in the average power of the interfering signals. This attenuates the increase in SINR, leading to a limited variation in p_c as λ increases in UC mode. In SFN mode, on the other hand, λ has a significant impact on p_c (Fig. 1), where we can see that the greater the λ, the higher the p_c. This difference can be explained by the fact that in SFN mode, the average useful power received increases more significantly than that of the average interference power.

Let us now compare p_c between UC and SFN transmission modes, focusing on a high SINR requirement (γ = 10 dB), as illustrated in Fig. 1. We can see that UC mode offers limited coverage, below 30%, whatever the values of λ and f_c. By contrast, SFN mode proves more advantageous, particularly when λ is higher. For example, for a density of 0.25 BS/km^2, the SFN mode offers a coverage probability varying between 67% and 83% (67% for f_{c3}, 73% for f_{c2}, and 83% for f_{c1}). With an increase in BS density to 2 BS/km^2, a 100% coverage probability is guaranteed, irrespective of f_c. Thus, the results in Fig. 1 to 3 highlight the effectiveness of synchronized transmission in SFN mode in reducing interference and increasing coverage, particularly in dense network deployments. These findings suggest that synchronization and inter-cell cooperation via SFN mode should be considered systematically to cope with network saturation in critical scenarios.

B. STRATEGY FOR IMPROVING THE COVERAGE PROBABILITY OF THE UC MODE BY BEAMFORMING

We now turn to strategies for improving the coverage probability p_c in conventional UC mode beyond the limits reached for all values of f_c and λ. To do this, we evaluate the conventional UC mode in combination with beamforming, characterized by a linear antenna array consisting of M antennas per sector of tri-sector BSs. Note that the simulations in Fig. 1 to 3 were performed with a single antenna per BS sector. Fig. 4 to 6 examine the impact of using 8 antennas (M = 8) on p_c, the average power of the useful signal received, and the average power of interference signals, respectively. These results allow us to better understand the advantages of beamforming over conventional UC mode, as well as to compare this approach with SFN mode, enriching our ability to develop solutions that guarantee reliable mass transmission.

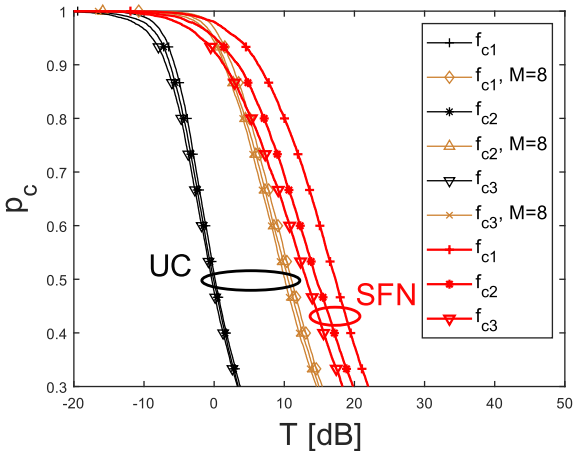

FIGURE 4. Coverage probability (p_c) in UC (with and without beamforming) and SFN modes, as a function of target SINR (T), for transmission power P_{tx} = 0.5 W, BS density λ = 0.25 BS/km^2, and three carrier frequencies (f_{c1} = 1.6 GHz, f_{c2} = 2 GHz, and f_{c3} = 2.4 GHz).

Fig. 4 clearly shows the benefits of beamforming over conventional UC mode, for λ = 0.25 BS/km^2. More precisely, there is an increase in p_c from M = 1 to M = 8, mainly due to the increase in the power of the useful signal received, accompanied by a significant limitation of the increase in the average power of interference signals, as illustrated in Fig. 5 and 6 for the three f_c values. These improvements in SINR contribute strongly to the increase in p_c in UC mode with beamforming when M is increased. However, it is important to note that even with M = 8, transmission in SFN mode remains more relevant to ensure better coverage.

Let us now compare p_c between the two modes for a target SINR (T) of 10 dB (Fig. 4). We see that in the case of UC mode, p_c varies from less than 30% for M = 1, to between 52% and 57% for M = 8 (52% for f_{c3}, 54% for f_{c2}, and 57% for f_{c1}). However, SFN mode is still more advantageous than UC mode, even with 8 antennas per sector, guaranteeing

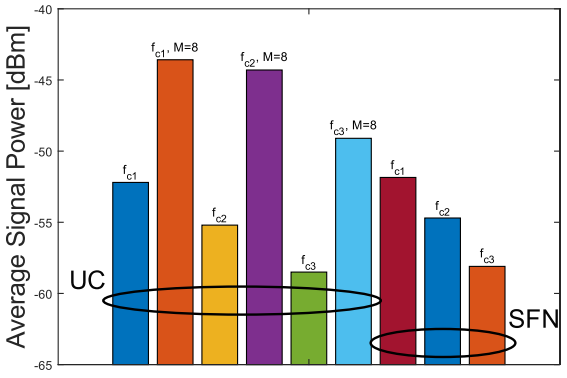

FIGURE 5. Average power of the useful signal received in UC (with and without beamforming) and SFN modes, for transmission power P_{tx} = 0.5 W, BS density $\lambda = 0.25$ BS/km^2, and three carrier frequencies (f_{c1} = 1.6 GHz, f_{c2} = 2 GHz, and f_{c3} = 2.4 GHz).

coverage of between 60% and 80% depending on the f_c value. This observation confirms the effectiveness of the SFN technique in reducing total interference compared with the UC mode, in line with the results of Fig. 1 to 3. In summary, this finding remains valid even when the UC mode is used with beamforming, as illustrated in Fig. 4 to 6.

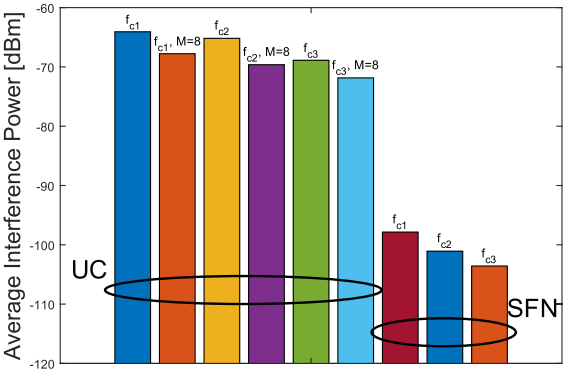

FIGURE 6. Average power of interference signals in UC (with and without beamforming) and SFN modes, for transmission power P_{tx} = 0.5 W, BS density $\lambda = 0.25$ BS/km^2, and three carrier frequencies (f_{c1} = 1.6 GHz, f_{c2} = 2 GHz, and f_{c3} = 2.4 GHz).

C. IMPACT OF TRANSMISSION POWER ON COVERAGE PROBABILITY IN UC AND SFN MODES

We now evaluate the impact of P_{tx} on p_c, as illustrated in Fig. 7, while maintaining a BS density $\lambda = 0.25$ BS/km^2, similar to that considered in Fig. 4 to 6. Fig. 7 explicitly highlights that an increase in P_{tx} from 0.5 W to 2 W results in a significant improvement in p_c in broadcast mode for all three f_c values, in contrast to UC mode where no significant improvement in p_c is observed above 0.5 W (for all three f_c values). Fig. 7 also highlights the p_c improvements offered by SFN mode when P_{tx} is increased from 0.5 W to 2 W. More precisely, comparing these gains for $\gamma = 10$ dB, we see that these improvements lead to coverage of between 60% and 80% for $P_{tx} = 0.5$ W, whereas for $P_{tx} = 2$ W, the improvements are even more marked, varying between 80%

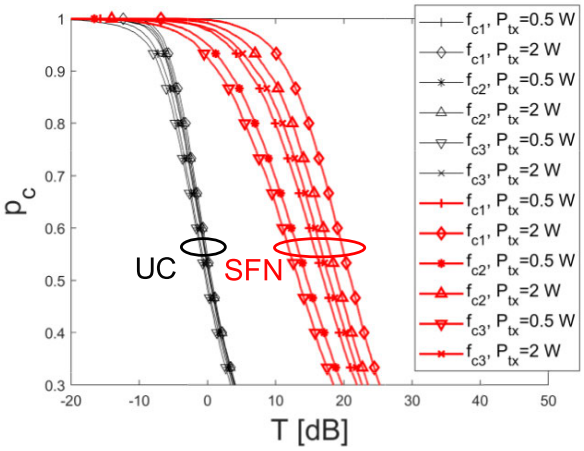

FIGURE 7. Coverage probability (p_c) in conventional UC and SFN modes, as a function of target SINR (T), for BS density $\lambda = 0.25$ BS/km^2, three carrier frequencies (f_{c1} = 1.6 GHz, f_{c2} = 2 GHz, and f_{c3} = 2.4 GHz), and two transmission powers P_{tx} = 0.5 W and 2 W.

and 94%, depending on the value of f_c. Thus, SFN mode transmission demonstrates its superiority over UC mode for the provision of large-scale emergency alerts, this time from an energy point of view. In this context, BSs provide better coverage than UC mode when transmitting in SFN broadcast mode, thanks to synchronization and cooperation between BSs, while having the advantage of transmitting at lower power.

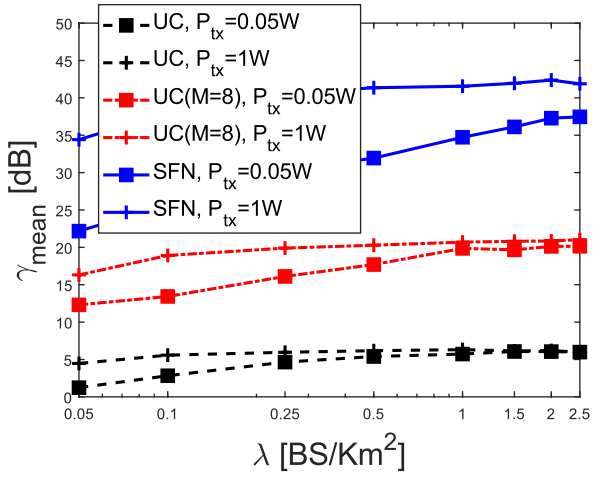

FIGURE 8. Average SINR (γ_{mean}) in conventional UC, UC with beamforming ($M = 8$) and SFN modes as a function of BS density (λ), for carrier frequency f_c=f_{c2}, and two transmission power values (P_{tx} = 0.05 W and 1 W).

D. AVERAGE SINR IN CONVENTIONAL UC, UC WITH BEAMFORMING AND SFN MODES

We now focus on evaluating the system's performance, using the mean SINR (γ_{mean}) as a criterion. The mean SINR is defined as the average SINR value obtained from the 10^4 Monte Carlo simulations. Fig. 8 shows the evolution of γ_{mean} as a function of BS density (λ) varying from 0.05 BS/km^2

to 2.5 BS/km^2, for carrier frequency $f_c = f_{c2}$, and two transmission power levels ($P_{tx} = 0.05$ W and 1 W). It is clear that increasing transmission power from 0.05 W to 1 W leads to a significant increase in γ_{mean}, particularly in SFN mode, compared to UC mode with beamforming (with $M = 8$), and even more so compared to conventional UC mode, where saturation sets in more quickly. For example, when P_{tx} is increased from 0.05 W to 1 W with $\lambda = 0.5$ BS/km^2, we see an increase in γ_{mean} from 5.4 dB to 6.2 dB in UC mode, from 17.7 dB to 20.3 dB in UC mode with beamforming (with $M = 8$), whereas in SFN, γ_{mean} increases from 31.9 dB to 40.6 dB.

On the other hand, by examining the ideal compromise between average SINR (γ_{mean}) and key system parameters, such as BS density (λ) and transmission power (P_{tx}), we find that this compromise is reached for a certain threshold value of λ. Beyond this value, the γ_{mean} shows no significant improvement for the different modes. For example, for $P_{tx} =$ 0.05 W, we obtain a compromise close to the optimum for $\lambda = 0.1$ BS/km^2 in UC mode, $\lambda = 0.25$ BS/km^2 in UC mode with beamforming (with $M = 8$), and $\lambda = 0.5$ BS/km^2 in SFN mode. This observation highlights the importance of the choice of BS density for achieving optimum system performance, while underlining the distinct advantages of conventional UC, UC with beamforming and SFN modes under different deployment conditions.

E. SWITCHING THRESHOLD AS A FUNCTION OF BS TRANSMISSION POWER FOR NORMALIZED SFN ZONE SIZE $\rho = 1$

Continuing our comparative analysis of transmission mode performance, we now turn our attention to evaluating the switching threshold ($N_{UC/BC}$), defining the number of users per BS beyond which broadcast modes (SFN and PTM) outperform UC mode (with and without beamforming) in terms of resource allocation. This evaluation is based on SINR and resource allocation results obtained from 10^4 Monte Carlo simulations, each describing a random distribution of BSs in the study area. The sensitivity of the threshold number of users $N_{UC/BC}$ to the variability of system parameters is a fundamental issue, which we examine below under different conditions.

Fig. 9 shows the switching threshold $N_{UC/BC}$ as a function of P_{tx}, varying from 0.05 W to 20 W, with different values of M from 1 to 32, as well as a BS density $\lambda = 0.25$ BS/km^2, a coverage requirement $p_c = 90\%$ and a normalized SFN zone size $\rho = 1$. These results highlight that increasing P_{tx} from 0.05 W to 20 W leads to a reduction in the $N_{UC/BC}$ threshold, reinforcing the value of switching to broadcast mode (from SFN or PTM) for more efficient resource use. As seen in Fig. 7 and 8, increasing P_{tx} considerably increases coverage and average SINR in broadcast mode, unlike in UC mode, where the power of interference signals predominates over the useful power received, thus limiting the improvement in coverage and average SINR in UC mode. Thus, an increase

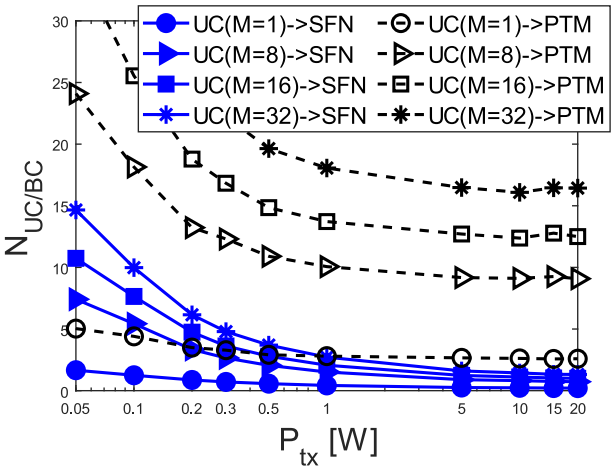

FIGURE 9. Switching threshold ($N_{UC/BC}$) for transition from UC mode (with and without beamforming) to broadcast mode (SFN and PTM), as a function of BS transmission power (P_{tx}), for carrier frequency f_c=f_{c2}, BS density $\lambda = 0.25$ BS/km^2, coverage requirement p_c= 90 %, and normalized SFN zone size $\rho = 1$.

in P_{tx} favors a faster transition to broadcast mode (SFN or PTM), requiring fewer and fewer users to activate this mode.

Fig. 9 also highlights the fact that the switching threshold $N_{UC/BC}$ increases with M. In correlation with the results in Fig. 4 to 6, increasing M leads to significantly higher useful receive power (with little change in interference power), which considerably improves SINR in UC mode with beamforming compared with conventional UC mode. Thus, the advantage of this mode is reinforced over the (SFN or PTM) mode, and in other words, switching to broadcast mode becomes less frequent as M increases, requiring a greater number of users to activate this mode.

Analysis of the thresholds for the transition from UC mode with beamforming ($M = 8, 16, 32$) to PTM and SFN broadcast modes reveals some striking developments. SFN switching curves show lower thresholds than those leading to PTM, indicating a faster transition and requiring fewer users to activate SFN. This observation underlines the crucial importance of the choice of broadcast mode between PTM and SFN from a resource allocation point of view, taking into account P_{tx} and M.

Let us now focus on the analysis of $N_{UC/BC}$ thresholds, examining the cases of low and high transmission power P_{tx}. The results in Fig. 9 can be summarized as follows:

- For low power levels, such as, for example, $P_{tx} = 0.1$W, switching to SFN mode requires at least 1 user per BS when $M = 1$, 6 users when $M = 8$, 8 users when $M = 16$, and 10 users when $M = 32$. To switch to PTM mode, more users are required: 5 when $M = 1$, 18 when $M = 8$, 26 when $M = 16$, and 33 when $M = 32$, all requesting the same content.
- For high power levels, such as $P_{tx} > 5$ W, switching to SFN mode requires only 1 user per BS, regardless of M in UC mode. On the other hand, switching to PTM mode requires more users as M increases: at least 3 users

per BS when $M = 1$, 9 users per BS when $M = 8$, 13 users per BS when $M = 16$, and 17 users per BS when $M = 32$.

F. SWITCHING THRESHOLD AS A FUNCTION OF COVERAGE REQUIREMENTS FOR NORMALIZED SFN ZONE SIZE $\rho = 1$

It's essential to emphasize that coverage requirements (p_c) play a central role in communications network planning, as they significantly influence the threshold number of users $N_{UC/BC}$ required to switch from UC mode (with or without beamforming) to broadcast mode (SFN or PTM). The $N_{UC/BC}$ thresholds shown in Fig. 9 are calculated to meet a coverage requirement of 90% of users. Thus, any change in this requirement will require recalculation of the $N_{UC/BC}$ thresholds, as illustrated in Fig. 10, which explores the evolution of this threshold as a function of p_c for different values of M.

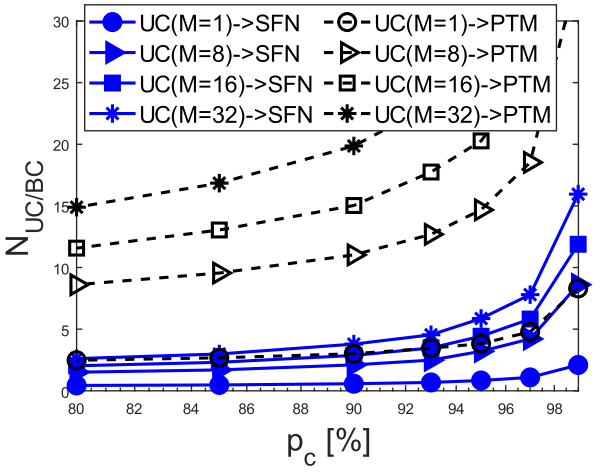

FIGURE 10. Switching threshold ($N_{UC/BC}$) for transition from UC mode (with and without beamforming) to broadcast mode (SFN and PTM), as a function of coverage requirement (p_c), for carrier frequency f_c=f_{c2}, BS density $\lambda = 0.25$ BS/km^2, BS transmission power P_{tx} = 0.5 W, and normalized SFN zone size $\rho = 1$.

The need to adjust the SINR target value, particularly in critical situations where signal quality must be maintained at an adequate level, stems from the fundamental need to ensure extensive coverage. This requirement is influenced by various scenarios and deployment conditions where guaranteeing safety remains a priority. The resulting considerations are of paramount importance, as the determination of $N_{UC/BC}$ thresholds and the adaptation of the target SINR value in response to channel conditions are both essential elements in guaranteeing effective reception of the alert content stream broadcast to users. These aspects are further explored in Fig. 10, which shows $N_{UC/BC}$ as a function of p_c for a BS density $\lambda = 0.25$ BS/km^2, a BS transmission power $P_{tx} = 0.5$ W, and a normalized SFN area size $\rho = 1$. Fig. 10 highlights that increasing the coverage requirement p_c, expressed by reducing the target SINR, results in an increase in the threshold $N_{UC/BC}$. This means that a stricter coverage requirement (high p_c) imposes a lower target SINR threshold in broadcast mode, delaying the switching phase to this mode and requiring greater user participation to activate this transition.

Furthermore, analysis of $N_{UC/BC}$ transition thresholds for different p_c, values, as illustrated in Fig. 10, reveals several interesting conclusions:

- For a very high coverage requirement, such as, for example, $p_c = 97\%$, SFN mode becomes more advantageous than UC mode for a number of users per BS ranging from 1 to 8, depending on the value of M in UC mode. On the other hand, PTM mode becomes more advantageous than UC mode as soon as there are 5 users per BS when $M = 1$, 19 users per BS when $M = 8$, 26 users per BS when $M = 16$, and 34 users per BS when $M = 32$, all requesting the same content.
- For a lower coverage requirement, such as, for example, $p_c = 80\%$, SFN mode becomes more advantageous than UC mode for a limited number of users per BS, ranging from 1 to 3, depending on the value of M between 1 and 32 in UC mode. On the other hand, PTM mode outperforms UC mode when the number of users per BS is higher, i.e. at least 3 users per BS when $M = 1$, 9 users per BS when $M = 8$, 12 users per BS when $M = 16$, and 15 users per BS when $M = 32$.

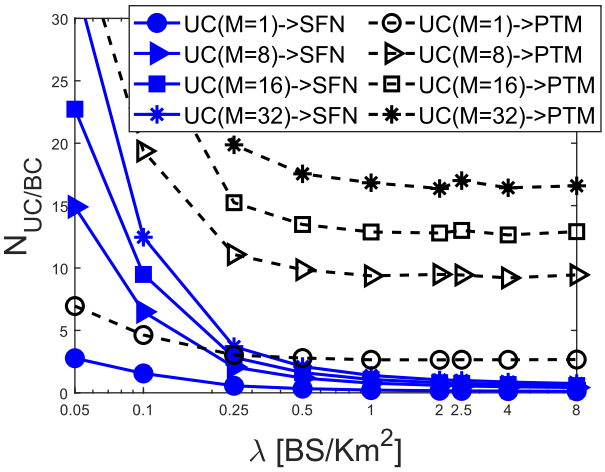

FIGURE 11. Switching threshold ($N_{UC/BC}$) for transition from UC mode (with and without beamforming) to broadcast mode (SFN and PTM), as a function of as a function of BS density (λ), for carrier frequency f_c=f_{c2}, BS transmission power P_{tx} = 0.5 W, coverage requirement p_c= 90%, and normalized SFN zone size $\rho = 1$.

G. SWITCHING THRESHOLD AS A FUNCTION OF BS DENSITY FOR NORMALIZED SFN ZONE SIZE $\rho = 1$

Continuing our analysis, we now examine the impact of BS density on the switching threshold, varying its λ value from 0.05 BS/km^2 to 8 BS/km^2, as illustrated in Fig. 11. The aim of this analysis is to assess how network densification affects the sensitivity of different modes in terms of resource allocation in the face of inter- and intra-cell interference. The results underline a decrease in $N_{UC/BC}$ with increasing

λ, highlighting a greater interest in broadcast modes (PTM and SFN) than in UC mode. This result can be explained by the fact that, unlike UC mode, where SINR improvement is restricted due to the increasing interference associated with high λ, PTM and SFN broadcast modes have the advantage of improving worst-case SINR more significantly with increasing λ, while using fewer resources in broadcast mode.

We now focus our attention on the analysis of $N_{UC/BC}$ switching thresholds, taking a close look at the scenarios associated with low and high λ. The results highlighted in Fig. 11 can be summarized as follows:

- At low λ, for example, $\lambda = 0.25$ BS/km^2, broadcast modes (SFN and PTM) generally outperform UC mode in terms of resource allocation, particularly in scenarios involving low and high values of the threshold number of users $N_{UC/BC}$. More specifically, switching can occur at a low level of $N_{UC/BC}$, when $M = 1$ for UC mode. On the other hand, this switching threshold increases significantly with increasing M. For example, the threshold rises from 10 users per BS when $M = 8$, to 13 users per BS when $M = 16$, and to 17 users per BS when $M = 32$, all requesting the same content.
- For a high λ, as in the case of $\lambda = 4$ BS/km^2, SFN mode becomes more advantageous than UC mode as soon as there is at least one user per BS. As for PTM mode, it becomes more advantageous than UC mode when the number of users per BS reaches 3 for $M = 1$, 9 for $M = 8$, 13 for $M = 16$, and 16 for $M = 32$, with all users requesting the same content.

H. SWITCHING THRESHOLD AS A FUNCTION OF BS TRANSMISSION POWER FOR NORMALIZED SFN ZONE SIZE $\rho \leq 1$

It should be noted that Fig. 9 to 11 depict an ideal scenario where all BSs in the study area operate in all four transmission modes (conventional UC, UC with beamforming, SFN, and PTM). In this configuration, the coverage area of BSs transmitting in SFN mode is assumed to encompass the entire study area, representing a normalized value of SFN area size $\rho = \frac{N_{SFN}}{N_{BS}} = 1$. However, under more realistic conditions, only a subset of BSs participates in synchronized cooperative transmission in SFN mode. In this case, BSs outside this zone can potentially generate harmful interference. Taking these practical aspects into account in a complex operational context complicates the situation, which justifies the interest in evaluating $N_{UC/BC}$ under more realistic conditions. We extend this analysis by considering different values of ρ, as illustrated in Fig. 12 and 13, to better reflect the constraints and opportunities associated with a practical implementation of the SFN broadcast mode.

Let us now focus our attention on Fig. 12, which compares the switching threshold $N_{UC/BC}$ as a function of P_{tx} for different normalized values of SFN zone size ($\rho = 0.1$, 0.2, 0.5, 1), with the parameters $\lambda = 0.25$ BS/km^2 and $p_c = 90\%$. The results show that when ρ is less than 1,

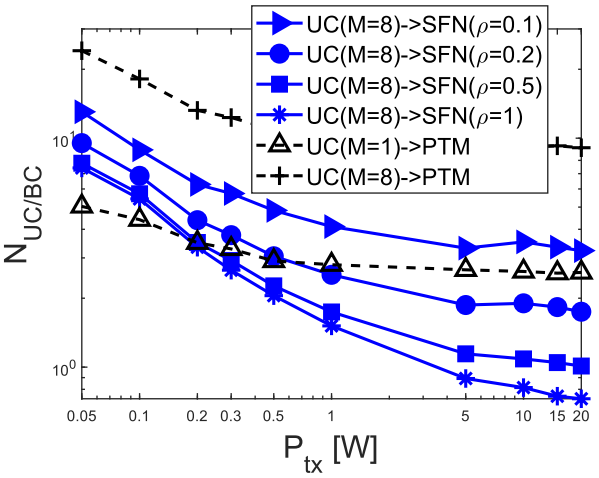

FIGURE 12. Switching threshold ($N_{UC/BC}$) for a transition from UC mode (with and without beamforming) to broadcast mode (SFN and PTM), as a function of P_{tx}, for f_c=f_{c2}, $\lambda = 0.25$ BS/km^2, p_c= 90%, and different normalized SFN zone sizes ($\rho = 0.1, 0.2, 0.5, 1$).

indicating that a group of BSs with a number N_{SFN} less than N_{BS} perform synchronized transmission in SFN mode, the switching threshold $N_{UC/BC}$ decreases slightly with increasing ρ. This observation confirms the advantages of broadcast mode via SFN over UC mode, even when the SFN zone does not cover the entire study area. This is because conventional UC mode, where each BS in the study area transmits independently, can lead to network congestion due to inter- and intra-cell interference. In contrast, SFN mode with ρ less than 1 reduces this congestion while guaranteeing efficient QoS for users, using fewer spectral resources.

In the analysis of the variation of the switching threshold $N_{UC/BC}$ as a function of ρ for $P_{tx} = 1$W in Fig. 12, the main results can be summarized as follows:

- For $\rho = 0.1$ (i.e. 10% of BS transmit in SFN), SFN broadcast mode becomes preferable to UC mode (with $M = 8$) when the number of users per BS exceeds 4.
- For $\rho = 0.2$ (i.e. 20% of BS transmit in SFN), SFN broadcast mode is preferred to UC mode (with $M = 8$) as soon as there are at least 3 users per BS.
- For $\rho = 0.5$ (i.e. 50% of BS transmit in SFN), SFN broadcast mode is favored over UC mode (with $M = 8$) as soon as there are at least 2 users per BS.
- PTM mode is favored over UC mode when there are at least 3 users per BS in UC mode (when $M = 1$), or at least 10 users per BS in UC mode (when $M = 8$), all requesting the same content.

A closer look at the switching curves in Fig. 12 for scenarios involving at least three users per BS reveals two distinct situations, highlighting the need for a transition to more spectrum-efficient broadcast modes:

- The first case occurs when P_{tx} is between 0.2 W and 1 W, marking the switch from conventional UC mode to PTM broadcast mode.
- The second case occurs when ρ is greater than or equal to 0.5 and P_{tx} is equal to 0.2 W, or when ρ reaches

0.2 and P_{tx} is between 0.5 W and 1 W. Under these conditions, the transition from UC mode with beamforming ($M = 8$) to SFN mode becomes imperative for optimum use of available resources.

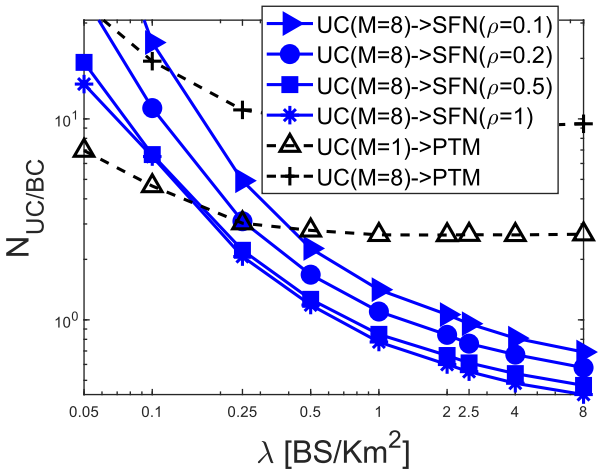

FIGURE 13. Switching threshold ($N_{UC/BC}$) for a transition from UC mode (with and without beamforming) to broadcast mode (SFN and PTM), as a function of λ, for f_c=f_{c2}, P_{tx}= 0.5 W, p_c= 90%, and different normalized SFN zone sizes (ρ = 0.1, 0.2, 0.5, 1).

I. SWITCHING THRESHOLD AS A FUNCTION OF BS DENSITY FOR NORMALIZED SFN ZONE SIZE $\rho \leq 1$

We conclude our study by examining, in Fig. 13, the impact of λ on the switching threshold $N_{UC/BC}$, maintaining the same values of ρ as considered in Fig. 12. To do this, we vary λ in the range 0.25 BS/km^2 to 8 BS/km^2, with the parameters $P_{tx} = 0.5$ W and $p_c = 90\%$. The main conclusions drawn from Fig. 13 can be summarized as follows:

- In the case of low BS density, such as $\lambda = 0.25$ BS/km^2, we find that, for identical content demand, switching from UC mode with beamforming ($M = 8$) to SFN mode requires at least: 2 users per BS when ρ exceeds 0.5, 3 users per BS when ρ equals 0.2, or 5 users per BS when ρ reaches 0.1. On the other hand, to make the transition to PTM broadcast mode, it is imperative to have at least 3 users per BS (when $M = 1$) or 11 users per BS (when $M = 8$).
- For high BS density, such as $\lambda = 4$ BS/km^2, switching from UC mode (with $M = 8$) to SFN broadcast mode is feasible as soon as there is at least one user per BS, whatever the value of ρ, which varies between 0.1 and 1. On the other hand, switching to PTM broadcast mode requires at least 2 users per BS (when $M = 1$) or 10 users per BS (when $M = 8$).

Finally, by analyzing the $N_{UC/BC}$ curves for scenarios involving at least three users per BS, we can identify two distinct cases that require SFN or PTM to switch to broadcast mode:

- The first case occurs when λ is between 0.15 BS/km^2 and 0.5 BS/km^2. In this range, for a given content demand, the transition from conventional UC mode (with $M = 1$) to PTM mode is imperative to optimize the use of spectrum resources.
- The second case arises when the normalized SFN zone size ρ reaches or exceeds 0.5, together with a BS density λ of 0.2 BS/km^2, or when ρ equals 0.2 and λ equals 0.25 BS/km^2, or when ρ is 0.1 and λ reaches 0.4 BS/km^2. In such configurations, for a given content demand, it is imperative to switch from UC mode with beamforming ($M = 8$) to SFN mode, for more efficient use of available resources.

J. SUMMARY OF SIMULATION RESULTS

Evaluation of the four transmission modes (conventional UC, UC with beamforming, PTM, and SFN), carried out using 10^4 Monte Carlo simulations, shows that the SFN mode stands out thanks to its high coverage probability (p_c) and SINR, particularly in networks with high BS density (λ) and high transmission power (P_{tx}), where its BS synchronization effectively mitigates inter-cell interference. Conversely, conventional UC mode provides the most limited coverage, while UC mode with beamforming significantly improves coverage without, however, reaching the performance of SFN mode.

The study also highlights the fact that the carrier frequency (f_c) mainly affects the UC mode with beamforming, whose efficiency decreases at higher frequencies, while the SFN mode remains the most resistant

Another crucial aspect of this analysis is the switching threshold $N_{UC/BC}$, which indicates the minimum number of users per BS required to justify the transition from UC mode (with or without beamforming) to broadcast modes (SFN or PTM). Simulation results show that this threshold varies significantly as a function of several system parameters (P_{tx}, λ, p_c, ρ, M):

- $N_{UC/BC}$ decreases as transmitted power P_{tx} increases, as coverage and SINR increase faster with P_{tx} in broadcast modes than in UC modes.
- $N_{UC/BC}$ increases when the coverage probability requirement p_c increases, because the corresponding SINR decreases faster with p_c in broadcast modes than in UC modes.
- $N_{UC/BC}$ decreases as the BS density λ increases, as broadcast modes are less affected by interference than UC modes.
- $N_{UC/BC}$ increases when normalized SFN zone size ρ decreases, due to SINR degradation in SFN mode.
- $N_{UC/BC}$ increases as the number of antennas M increases, because beamforming increases the useful power received and reduces interference variations, which improves SINR in UC. Furthermore, for a number of antennas $M \geq 8$ in UC mode with beamforming, $N_{UC/BC}$ is always lower in SFN mode than in UC mode.

K. LIMITATIONS AND SUGGESTIONS FOR FUTURE STUDIES

Although this study reveals essential elements about the performance of the four transmission modes, their scope remains

limited to the specific simulation conditions, depending in particular on the distribution and density of the BSs, the channel model, and the carrier frequencies. For instance, our results are based on simulations where BSs are randomly distributed according to PPP in a 20 km^2 square area, using carrier frequencies well below millimeter-wave (mmWave) and terahertz. As such, these findings may not be directly applicable to more complex urban environments, nor to 5G mmWave and 6G networks, which often feature increased heterogeneity, diversified antenna configurations, and more complex interference.

In order to deepen and broaden the scope of our findings, it would be useful to carry out further studies incorporating more diverse scenarios and network configurations. This would include heterogeneous networks, simultaneous delivery of different content, non-uniform BS distributions, dynamically adaptable active BS densities, and propagation models adapted to urban, suburban and rural environments. Simulations that also take into account different cell types (macro, micro and pico) would enable us to fine-tune the performance of the four transmission modes in various mass dissemination contexts.

VI. CONCLUSION

This article focused on the analysis of mechanisms to ensure reliable and efficient transmission within dense cellular networks, particularly in crisis or threat contexts. We focused on improving public safety through the mass dissemination of emergency downlink alert content, taking into account both inter- and intra-cellular interference. We examined the impact of various transmission modes, including conventional UC, UC with beamforming, SFN, and PTM, in real network environments characterized by the random distribution of BSs according to a PPP-type law. Our study analyzed in detail the performance of these modes in terms of coverage probability and resource utilization, providing recommendations for various scenarios and deployment conditions. In addition, we examined two distinct types of configurations: one in which the SFN zone encompasses the entire study area, and another in which only certain BSs in the study area, located around the point of origin, contribute to SFN broadcasting. Our simulation results confirm that broadcast transmission modes (SFN and PTM) outperform UC mode in terms of resource allocation when the number of users reaches a certain threshold. This threshold, identified in various scenarios, shows notable sensitivity to the variability of several key parameters, including the transmission power of BSs, their density, the number of antennas per sector, the normalized size of the SFN zone, and coverage requirements. This study is of crucial importance in guiding the design of future 5G and 6G networks, as it enables the optimum transmission mode to be chosen from PTM, SFN, conventional UC, and UC with beamforming, while taking into account inter- and intra-cellular interference. It is particularly relevant to meeting specific needs such as emergency alerts in dangerous situations, thereby improving public safety.

REFERENCES

[1] E. F. Pupo, C. C. Gonzalez, L. Atzori, and M. Murroni, "Dynamic multicast access technique in SC-PTM 5G networks: Subgrouping with OM/NOM," in *Proc. IEEE Int. Symp. Broadband Multimedia Syst. Broadcast. (BMSB)*, Bilbao, Spain, Jun. 2022, pp. 1–6.

[2] O. O. Erunkulu, A. M. Zungeru, C. K. Lebekwe, M. Mosalaosi, and J. M. Chuma, "5G mobile communication applications: A survey and comparison of use cases," *IEEE Access*, vol. 9, pp. 97251–97295, 2021.

[3] A. Ghosh, A. Maeder, M. Baker, and D. Chandramouli, "5G evolution: A view on 5G cellular technology beyond 3GPP release 15," *IEEE Access*, vol. 7, pp. 127639–127651, 2019.

[4] H. Arslan, S. Dogan Tusha, and A. Yazar, "6G vision: An ultra-flexible perspective," *ITU J. Future Evolving Technol.*, vol. 1, no. 1, pp. 121–140, Dec. 2020.

[5] W. U. Rehman, T. Salam, A. Almogren, K. Haseeb, I. U. Din, and S. H. Bouk, "Improved resource allocation in 5G MTC networks," *IEEE Access*, vol. 8, pp. 49187–49197, 2020.

[6] H. H. Yang, A. Arafa, T. Q. S. Quek, and H. V. Poor, "Optimizing information freshness in wireless networks: A stochastic geometry approach," *IEEE Trans. Mobile Comput.*, vol. 20, no. 6, pp. 2269–2280, Jun. 2021.

[7] Y. Hmamouche, M. Benjillali, S. Saoudi, H. Yanikomeroglu, and M. D. Renzo, "New trends in stochastic geometry for wireless networks: A tutorial and survey," *Proc. IEEE*, vol. 109, no. 7, pp. 1200–1252, Jul. 2021.

[8] K. Huang and J. G. Andrews, "A stochastic-geometry approach to coverage in cellular networks with multi-cell cooperation," in *Proc. IEEE Global Telecommun. Conf.*, Houston, TX, USA, Dec. 2011, pp. 1–5.

[9] M. A. Ouamri, M. Azni, and M.-E. Oteşteanu, "Coverage analysis in two-tier 5G hetnet based on stochastic geometry with interference coordination strategy," *Wireless Pers. Commun.*, vol. 121, no. 4, pp. 3213–3222, Dec. 2021.

[10] S. S. Kalamkar, F. M. Abinader, F. Baccelli, A. S. M. Fani, and L. G. U. Garcia, "Stochastic geometry-based modeling and analysis of beam management in 5G," in *Proc. IEEE Global Commun. Conf.*, Taipei, Taiwan, Dec. 2020, pp. 1–6.

[11] M. U. A. Siddiqui, F. Qamar, F. Ahmed, Q. N. Nguyen, and R. Hassan, "Interference management in 5G and beyond network: Requirements, challenges and future directions," *IEEE Access*, vol. 9, pp. 68932–68965, 2021.

[12] A. A. Salem, S. El-Rabaie, and M. Shokair, "Survey on ultra-dense networks (UDNs) and applied stochastic geometry," *Wireless Pers. Commun.*, vol. 119, no. 3, pp. 2345–2404, Aug. 2021.

[13] M. U. A. Siddiqui, H. Abumarshoud, L. Bariah, S. Muhaidat, M. A. Imran, and L. Mohjazi, "URLLC in beyond 5G and 6G networks: An interference management perspective," *IEEE Access*, vol. 11, pp. 54639–54663, 2023.

[14] J. Vargas, C. Thienot, and X. Lagrange, "MBSFN and SC-PTM as solutions to reduce energy consumption in cellular networks," in *Proc. IEEE Symp. Comput. Commun. (ISCC)*, Paris, France, Jun. 2022, pp. 1–6.

[15] A. Daher, M. Coupechoux, P. Godlewski, J.-M. Kelif, P. Ngouat, and P. Minot, "SINR model for MBSFN based mission critical communications," in *Proc. IEEE 86th Veh. Technol. Conf. (VTC-Fall)*, Sep. 2017, pp. 1–5.

[16] A. Alieldin, Y. Huang, M. Stanley, S. D. Joseph, and D. Lei, "A 5G MIMO antenna for broadcast and traffic communication topologies based on pseudo inverse synthesis," *IEEE Access*, vol. 6, pp. 65935–65944, 2018.

[17] I. Khalid, M. Girmay, V. Maglogiannis, D. Naudts, A. Shahid, and I. Moerman, "An adaptive MBSFN resource allocation algorithm for multicast and unicast traffic," in *Proc. IEEE 20th Consum. Commun. Netw. Conf. (CCNC)*, Las Vegas, NV, USA, Jan. 2023, pp. 579–586.

[18] *Mission Critical Services Common Requirements*, document TS 22.280, 3GPP, 2018.

[19] D. Mi, J. Eyles, T. Jokela, S. Petersen, R. Odarchenko, E. Öztürk, D.-K. Chau, T. Tran, R. Turnbull, H. Kokkinen, B. Altman, M. Bot, D. Ratkaj, O. Renner, D. Gomez-Barquero, and J. J. Gimenez, "Demonstrating immersive media delivery on 5G broadcast and multicast testing networks," *IEEE Trans. Broadcast.*, vol. 66, no. 2, pp. 555–570, Jun. 2020.

[20] P. Zhao, L. Feng, P. Yu, W. Li, and X. Qiu, "A social-aware resource allocation for 5G device-to-device multicast communication," *IEEE Access*, vol. 5, pp. 15717–15730, 2017.

[21] C. Shen, C. Liu, R. A. Rouil, and H.-A. Choi, "Study of multicast broadcast single frequency network area in multicast communications," in *Proc. 14th Int. Conf. Signal Process. Commun. Syst. (ICSPCS)*, Adelaide, SA, Australia, Dec. 2020, pp. 1–8.
[22] E. Garro, M. Fuentes, J. L. Carcel, H. Chen, D. Mi, F. Tesema, J. J. Gimenez, and D. Gomez-Barquero, "5G mixed mode: NR multicast-broadcast services," *IEEE Trans. Broadcast.*, vol. 66, no. 2, pp. 390–403, Jun. 2020.
[23] *Study on Application Architecture to Support Mission Critical Push To Talk Over LTE (MCPTT) Services*, document TR 23.779, 3GPP, 2015.
[24] A. Daher, M. Coupechoux, P. Godlewski, P. Ngouat, and P. Minot, "A dynamic clustering algorithm for multi-point transmissions in mission-critical communications," *IEEE Trans. Wireless Commun.*, vol. 19, no. 7, pp. 4934–4946, Jul. 2020.
[25] D. Jagyasi and M. Coupechoux, "Secure and robust MIMO transceiver for multicast mission critical communications," *IEEE Trans. Veh. Technol.*, vol. 71, no. 6, pp. 6351–6366, Jun. 2022.
[26] A. Awada, D. Navrátil, and M. Säily, "A study on single-cell point-to-multipoint transmission for public safety communications with eMBMS LTE networks," in *Proc. IEEE Wireless Commun. Netw. Conf.*, Doha, Qatar, Apr. 2016, pp. 1–6.
[27] M. Younes and Y. Louet, "Analysis of unicast/broadcast switch over with regard to resource allocation for future cellular networks," in *Proc. 4th Global Power, Energy Commun. Conf. (GPECOM)*, Cappadocia, Turkey, Jun. 2022, pp. 605–610.
[28] A. Alexiou, K. Asimakis, C. Bouras, V. Kokkinos, and A. Papazois, "Combining MBSFN and PTM transmission schemes for resource efficiency in LTE networks," in *Proc. Int. Conf. Wired/Wireless Internet Commun.*, Barcelona, Spain, Jun. 2011, pp. 56–67.
[29] A. Daher, M. Coupechoux, P. Godlewski, P. Ngouat, and P. Minot, "SC-PTM or MBSFN for mission critical communications?" in *Proc. IEEE 85th Veh. Technol. Conf. (VTC Spring)*, Sydney, NSW, Australia, Jun. 2017, pp. 1–6.
[30] Y. Zhang, D. He, Y. Xu, Y. Guan, and W. Zhang, "MBSFN or SC-PTM: How to efficiently multicast/broadcast," *IEEE Trans. Broadcast.*, vol. 67, no. 3, pp. 582–592, Sep. 2021.
[31] H. Chen, D. Mi, M. Fuentes, D. Vargas, E. Garro, J. L. Carcel, B. Mouhouche, P. Xiao, and R. Tafazolli, "Pioneering studies on LTE eMBMS: Towards 5G point–to-multipoint transmissions," in *Proc. IEEE 10th Sensor Array Multichannel Signal Process. Workshop (SAM)*, Jul. 2018, pp. 1–4.
[32] *Evolved Universal Terrestrial Radio Access (E-UTRA); Radio Frequency (RF) System Scenarios*, document TR 36.942, 3GPP, 2018.
[33] *Technical Specification Group Radio Access Network; Introduction of the MBMS in the Radio Access Network; Stage 2 (release 9)*, document TS 25.346, 3GPP, 2009.
[34] *Multimedia Broadcast/Multicast Service (MBMS) Architecture and Functional Description*, document TS 23.246, 3GPP, 2019.
[35] W. Ding, J. Wang, Y. Li, P. Mumford, and C. Rizos, "Time synchronization error and calibration in integrated GPS/INS systems," *ETRI J.*, vol. 30, no. 1, pp. 59–67, Feb. 2008.
[36] M. Säily, C. Barjau, D. Navrátil, A. Prasad, D. Gómez-Barquero, and F. B. Tesema, "5G radio access networks: Enabling efficient point-to-multipoint transmissions," *IEEE Veh. Technol. Mag.*, vol. 14, no. 4, pp. 29–37, Sep. 2019.
[37] *Study on Single-cell Point-to-Multipoint Transmission for E-UTRA*, document TR 36.890, 3GPP, 2015.
[38] V. K. Shrivastava, S. Baek, and Y. Baek, "5G evolution for multicast and broadcast services in 3GPP release 17," *IEEE Commun. Standards Mag.*, vol. 6, no. 3, pp. 70–76, Sep. 2022.
[39] J. J. Gimenez, P. Renka, S. Elliott, D. Vargas, and D. Gomez-Barquero, "Enhanced TV delivery with EMBMS: Coverage evaluation for rooftop reception," in *Proc. IEEE Int. Symp. Broadband Multimedia Syst. Broadcast. (BMSB)*, Valencia, Spain, Jun. 2018, pp. 1–5.
[40] *Interim Report From Email Discussion on 5G Broadcast Evolution*, document RP-180499, 3GPP, 2018.
[41] T. Tran, D. Navrátil, P. Sanders, J. Hart, R. Odarchenko, C. Barjau, B. Altman, C. Burdinat, and D. Gomez-Barquero, "Enabling multicast and broadcast in the 5G core for converged fixed and mobile networks," *IEEE Trans. Broadcast.*, vol. 66, no. 2, pp. 428–439, Jun. 2020.
[42] *Study on Scenarios and Requirements for Next Generation Access Technologies*, document TR 38.913, 3GPP, 2017.
[43] *Study on LTE-Based 5G Terrestrial Broadcast*, document TR 36.776, 3GPP, 2018.
[44] *Multimedia Broadcast/Multicast Service (MBMS) Improvements; MBMS Operation on Demand*, document TR 26.849, 3GPP, 2015.
[45] *Multimedia Broadcast/Multicast Service (MBMS); Protocols and Codecs*, document TS 26.346, 3GPP, 2015.
[46] T. Stevens, *Key Technologies for the Content Distribution Framework*, document Deliverable D5.2, 5G-PPP 5G-Xcast Project, 2019.
[47] L. Carla, R. Fantacci, F. Gei, D. Marabissi, and L. Micciullo, "LTE enhancements for public safety and security communications to support group multimedia communications," *IEEE Netw.*, vol. 30, no. 1, pp. 80–85, Jan. 2016.
[48] A. Othman and N. A. Nayan, "Public safety mobile broadband system: From shared network to logically dedicated approach leveraging 5G network slicing," *IEEE Syst. J.*, vol. 15, no. 2, pp. 2109–2120, Jun. 2021.
[49] R. Borralho, A. Mohamed, A. U. Quddus, P. Vieira, and R. Tafazolli, "A survey on coverage enhancement in cellular networks: Challenges and solutions for future deployments," *IEEE Commun. Surveys Tuts.*, vol. 23, no. 2, pp. 1302–1341, 2nd Quart., 2021.
[50] T. T. Vu, L. Decreusefond, and P. Martins, "An analytical model for evaluating outage and handover probability of cellular wireless networks," *Wireless Pers. Commun.*, vol. 74, no. 4, pp. 1117–1127, Feb. 2014.

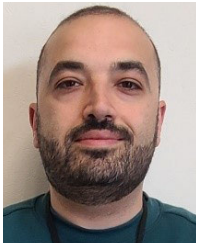

MOHAMAD YOUNES received the M.S. degree in electronics engineering and the M.S. degree in telecommunications research from Brest National School of Engineering (ENIB), Brest, France, in 2015, and the Ph.D. degree in digital communications from the University of Western Brittany (UBO), Brest, in 2019.

From 2019 to 2020, he was an Associate Professor with École Normale Supérieure (ENS), Rennes, France. From 2020 to 2022, he was a Postdoctoral Researcher with CentraleSupélec, Rennes. Since 2022, he has been an Associate Professor with the Military Academy of Saint-Cyr Coëtquidan (AMSCC) and a Researcher with the Coëtquidan Research Center. His research interests include digital communications, signal processing, wireless communications, and resource allocation for 5G/6G and LoRaWAN networks.

YVES LOUËT (Senior Member, IEEE) received the Ph.D. degree in digital communications and the Habilitation (HDR) degree in research from Rennes University, France, in 2000 and 2010, respectively. The topic of his Ph.D. thesis regarded peak to average power reduction in OFDM modulation with channel coding. He was a Research Engineer with SIRADEL Company, Rennes, in 2000, where he was involved in channel propagation modeling for cell planning. He was also involved in French collaborative research projects, including COMMINDOR, ERASME, and ERMITAGES about channel modeling in many frequency bands, especially 60 and five GHz for further telecommunication systems. In 2002, he joined Supélec as an Associate Professor. In 2010, he was a Full Professor with Supélec and later CentraleSupélec. He is currently the Head of the Signal Communication Embedded Electronics Research Group, CNRS, Institute of Electronics and Telecommunications, Rennes Laboratory; and the President of the URSI Commission C. His teaching and research activities were in line with signal processing and digital communications applied to software and cognitive radio systems. He was involved in many collaborative European projects, including FP7E2R, CELTIC B21C, CELTIC SHARING, NoE Newcom, and COST; and French projects, including ANR PROFIL, ANR INFOP, WONG5, FUI AMBRUN, APOGEES, TEPN, and WINOCOD. His research contribution is mainly focused on new waveforms designed for green cognitive radio and energy efficiency enhancement.